processes

MDPI

Article

Effects of Pyrolysis Temperature and Simulated Formation Stress on Tar Yield and Composition of Tar-Rich Coal

Honglun Cong [1], Wenfeng Wang [1,2,3,*] and Hayierhan Shadaitihan [4]

[1] College of Geology and Mining Engineering, Xinjiang University, Urumqi 830017, China
[2] School of Resources and Geosciences, China University of Mining and Technology, Xuzhou 221116, China
[3] Key Laboratory of Coalbed Methane Resources and Reservoir Formation Process, Ministry of Education, China University of Mining and Technology, Xuzhou 221008, China
[4] Zhundong Economic and Technological Development Zone Branch, Natural Resources Bureau of Changji Hui Autonomous Prefecture, Changji 831700, China
* Correspondence: wangwenfeng@cumt.edu.cn

Abstract

To clarify the effects of pyrolysis temperature and simulated formation stress on the tar yield and composition of Baishihu tar-rich coal, lump coal pyrolysis experiments were conducted using coal from the Baishihu Mine in the Naomaohu mining area, Xinjiang, at pyrolysis temperatures of 200–700 °C under no external stress and 15 MPa simulated formation stress conditions. Product yields were analyzed, and the chemical composition of tar was characterized using gas chromatography–mass spectrometry (GC–MS), with component abundances expressed as normalized relative peak areas. The results showed that the maximum tar yields were obtained at 400 °C under both stress conditions, reaching 9.53% and 8.81%, respectively. With increasing temperature, tar composition exhibited a stagewise evolution: oxygen-containing compounds were relatively enriched at low temperatures; aliphatic hydrocarbons showed a high relative peak area proportion at 400 °C; monocyclic aromatic hydrocarbons became significantly enriched at 500 °C; and the tar composition further evolved toward polycyclic aromatic structures at high temperatures. The 15 MPa simulated formation stress decreased the tar yield at 400 °C but altered the internal component distribution of tar, resulting in the relative enrichment of aromatic components. The results indicate that pyrolysis temperature and simulated formation stress jointly influence tar composition evolution of Baishihu tar-rich coal, and 400–500 °C represents a temperature range of particular interest for Baishihu tar-rich coal pyrolysis.

Keywords: tar-rich coal; pyrolysis; tar composition; fractionated utilization

Check for updates

Academic Editor: Ye Huang

Received: 23 September 2026
Revised: 21 October 2026
Accepted: 29 October 2026
Published: 3 November 2026

Copyright: © 2026 by the authors. Licensee MDPI, Basel, Switzerland. This article is an open access article distributed under the terms and conditions of the Creative Commons Attribution (CC BY) license.

1. Introduction

Coal pyrolysis is an important coal-conversion process in which coal organic matter undergoes cracking and restructuring upon heating under oxygen-free or oxygen-limited conditions, producing gaseous products, liquid tar, and solid semi-coke [1]. Tar-rich coal has a relatively high potential for tar generation, and pyrolysis can preferentially recover oil and gas components from coal, thereby enabling a transition from direct combustion toward the integrated utilization of oil, gas, and chemical products [2–6]. Tar-rich coal is generally classified according to the tar yield obtained from low-temperature carbonization tests. Coal with a tar yield of ≥7 wt% is considered a tar-rich coal resource. Tar-rich coal resources are abundant in western China, and their oil-and-gas resource attributes and development potential have attracted extensive attention [2–4]. Coal tar, an important liquid product of

 https://doi.org/10.3390/pr14213549

tar-rich coal pyrolysis, is a complex mixture containing aliphatic hydrocarbons, aromatic hydrocarbons, phenols, ketones, and other oxygen-containing compounds; these components differ substantially in processing characteristics and potential utilization value [7,8]. Therefore, in addition to improving tar yield, clarifying how pyrolysis conditions regulate tar composition and the distribution of target compounds is essential for evaluating the utilization performance of tar-rich coal.

Underground in situ pyrolysis directly heats tar-rich coal within the coal seam, allowing the generated oil and gas products to migrate through pores and fractures and be recovered at the surface. This approach can reduce conventional coal mining, transportation, and large-scale surface pyrolysis operations and is therefore regarded as an important route for developing the oil-and-gas resources of tar-rich coal. In recent years, substantial research has been conducted on borehole-based in situ pyrolysis, convective heating, microwave heating, and other underground heating technologies [5,9–14]. However, unlike surface pyrolysis, underground coal is continuously constrained by formation stress. Heating is also accompanied by coal-matrix shrinkage, pore–fracture evolution, and volatile transport, making product generation and release under in situ conditions more complex [15,16]. Consequently, temperature and formation stress may affect not only tar generation but also volatile migration and residence within the coal matrix, thereby influencing secondary cracking, cyclization, and aromatization reactions. Pyrolysis temperature is a key factor controlling the extent of organic-structure decomposition and product distribution, while pressure conditions can also alter coal pyrolysis behavior. Previous studies have shown that coal-pyrolysis product yields and semi-coke structures vary under different gas-pressure conditions [17–21]. More recent studies under simulated in situ conditions further indicate that stress level can influence tar and gas production, pore–fracture structure, and volatile transport [22–26]. However, previous studies on pressure effects have primarily focused on the influence of gas pressure within the reaction system, whereas coal seams under in situ conditions are subjected to mechanical formation stress as an external constraint. These two pressure conditions differ fundamentally in their loading mechanisms and their influences on the migration and retention behavior of volatile products. In addition, differences in coal-forming environment and molecular structure can significantly affect the pyrolysis behavior and tar-generation potential of tar-rich coal [27,28]. For lump tar-rich coal, the effects of mechanical formation stress on the temperature-dependent evolution of tar yield, chemical composition, and light aromatic components remain insufficiently understood. In particular, under simulated in situ pyrolysis conditions, it remains unclear whether formation stress can regulate tar composition by altering the residence time of volatile products and subsequent secondary reaction processes. From the perspective of resource utilization, tar yield alone is insufficient for evaluating in situ pyrolysis performance; tar quantity and composition should be considered together to identify the dominant product characteristics under different pyrolysis conditions and to support subsequent fractionated utilization.

The Baishihu coal from the Naomaohu mining area in Xinjiang has favorable tar-rich coal characteristics and is a representative target for in situ oil-and-gas recovery [29]. Based on the above considerations, lump coal samples from the Baishihu Mine were selected for pyrolysis experiments at 200, 300, 400, 500, 600, and 700 °C. Axial and confining mechanical stresses of 15 MPa were applied to simulate the formation stress environment. This stress condition represents the mechanical constraint experienced by coal seams during underground development and is distinguished from the gas pressure within the reaction system. The yields of semi-coke, gas, water, and tar were determined, and the tar composition was characterized by GC–MS. The identified valid components were classified as saturated aliphatic hydrocarbons, unsaturated aliphatic hydrocarbons, monocyclic aromatic

hydrocarbons, polycyclic aromatic hydrocarbons, phenols, other oxygen-containing compounds, and N/S-containing heteroatom compounds. The effects of pyrolysis temperature and simulated formation stress on tar yield and composition were investigated, and potential fractionated-utilization routes for tar produced at different temperatures were further discussed. The aim was to reveal the temperature-dependent evolution and simulated formation-stress response of Baishihu tar-rich coal tar, thereby providing an experimental basis for optimizing in situ pyrolysis conditions and directing liquid-product utilization.

2. Materials and Methods

2.1. Coal Sample

The coal samples used in this study were collected from the No. 1 coal seam of the Baishihu Open-pit Coal Mine in the Naomaohu mining area, Xinjiang, China. Lump coal samples were used for the pyrolysis experiments. According to the dimensions of the experimental apparatus, the raw coal was processed into two cylindrical specimens with a diameter of approximately 10 cm and a length of approximately 11 cm (Figure 1). The initial masses of the two coal specimens were recorded as 1083 g and 1106.5 g, respectively. In addition, a portion of the raw coal sample was crushed and ground to below 200 mesh, followed by vacuum drying at 50 °C for 24 h, and then used for proximate and ultimate analyses. The proximate and ultimate analyses were conducted according to the Chinese standards GB/T 212-2008 [30] and GB/T 476-2008 [31], respectively. The analysis results are presented in Table 1.

Table 1. Proximate and ultimate analyses of Baishihu coal.

Sample	Proximate Analysis (%)			Ultimate Analysis (%)				
	M_{ad}	A_d	V_{daf}	C_{daf}	H_{daf}	H_{ad}	N_{daf}	$O_{daf} + S_{daf}$
1	8.91	10.76	51.28	73.57	5.44	4.14	1.55	19.44
2	9.5	10.14	50.01	73.64	5.02	4.08	1.55	19.79
3	9	10.67	50.29	73.92	5.36	4.16	1.52	19.2

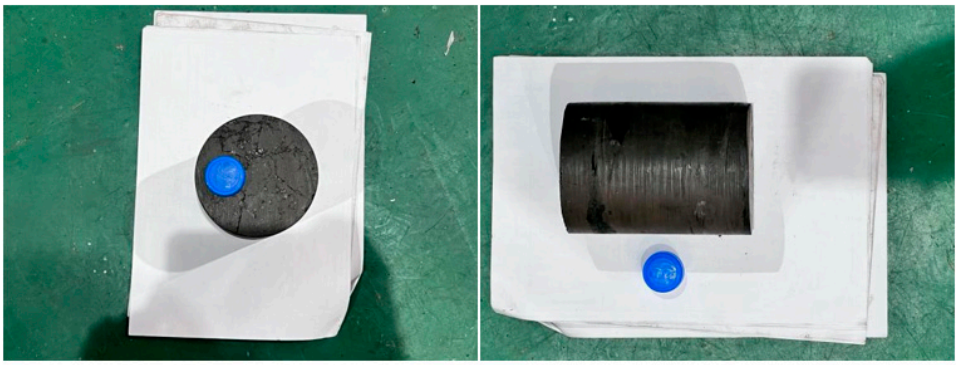


Figure 1. Coal samples used in the pyrolysis experiments.

2.2. Pyrolysis Experiments

Pyrolysis experiments were conducted using a self-designed in situ pyrolysis simulation apparatus (Nantong, China), as shown in Figure 2. The cylindrical coal specimens were placed inside the reaction chamber, and axial pressure and confining pressure were applied through a loading control system to simulate the formation stress environment experienced by coal seams during in situ pyrolysis. Two experimental conditions were considered in this study: (1) no-external-stress condition, and (2) simulated formation

stress condition, in which both axial pressure and confining pressure were maintained at 15 MPa. The 15 MPa simulated formation-stress condition was selected with reference to the typical mechanical confinement environment of shallow-to-medium-depth coal seams in the study area (approximately 600 m burial depth) and was used to investigate the effects of mechanical stress constraints on pyrolysis product generation and compositional evolution of tar-rich coal. It should be noted that the staged pyrolysis experiments were conducted only once under each of the two stress conditions, without independent replicates.

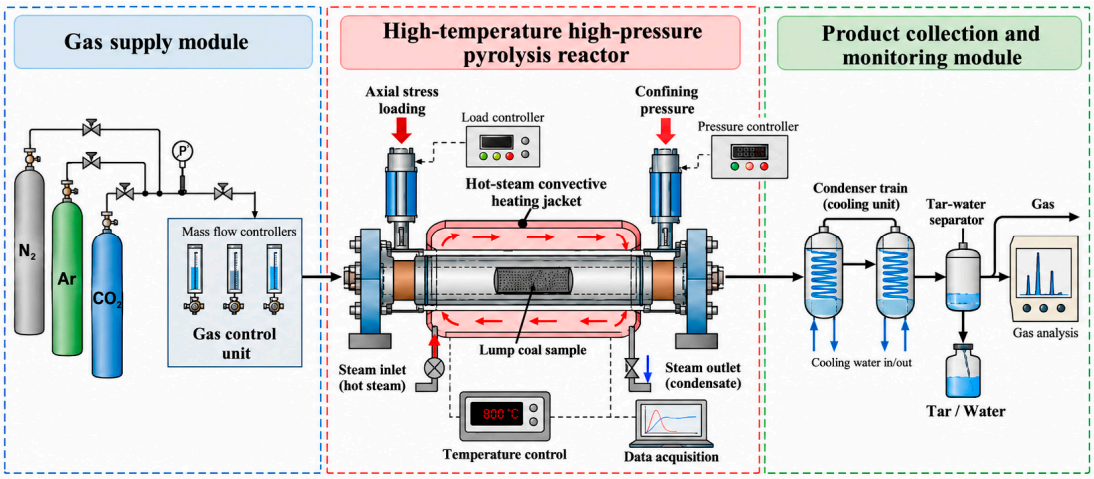


Figure 2. Experimental apparatus for simulating in situ pyrolysis.

Before each experiment, the coal specimen was installed in the reaction chamber, followed by stress loading. The specimen was then heated to the target temperature at a heating rate of 10 °C/min. The lump coal sample was continuously heated from 200 to 700 °C, and gaseous and condensed products were collected at different temperature intervals (200, 300, 400, 500, 600, and 700 °C). After reaching the target temperature, the sample was maintained for 4 h to ensure sufficient heat transfer within the lump coal specimen and completion of the pyrolysis process. The same holding time was applied for all temperature conditions to minimize the influence of residence time differences on tar composition evolution. During pyrolysis, high-purity nitrogen was introduced to provide an inert pyrolysis atmosphere. Prior to the heating stage of the pyrolysis experiment, nitrogen (N_2) was introduced into the reactor at an injection pressure of 2 MPa and a flow rate of 1 mL/min. The gaseous products, condensed liquid products, and solid residues generated during pyrolysis were collected separately.

Because a continuous heating procedure was adopted in this study, the product yields at each temperature stage were calculated based on the mass of the semi-coke obtained from the previous temperature stage rather than the initial coal mass. The yield of each product was calculated as follows:

$$Y_i = \frac{m_i}{m_{\mathrm{char},i-1}} \times 100\%$$

where Y_i is the yield of product i at the current temperature stage (%), m_i is the mass of the corresponding product obtained at the current stage (g), and $m_{\mathrm{char},i-1}$ is the mass of semi-coke obtained from the previous temperature stage (g).

The mass of non-condensable gaseous products and unrecovered losses was estimated by mass balance as follows:

$$m_{\mathrm{gas+loss}} = m_0 - m_{\mathrm{semi-coke}} - m_{\mathrm{tar}} - m_{\mathrm{water}}$$

Accordingly, the gas + loss yield was calculated as follows:

$$Y_{\text{gas+loss}} = \frac{m_{\text{gas+loss}}}{m_0} \times 100\% = 100\% - Y_{\text{semi-coke}} - Y_{\text{tar}} - Y_{\text{water}}$$

where $m_{\text{gas+loss}}$ is the mass of non-condensable gaseous products and unrecovered losses at the current temperature stage (g); m_0 is the mass of the sample at the beginning of the current temperature stage (g), corresponding to the semi-coke mass remaining from the preceding stage in the continuous-heating experiment; $m_{\text{semi-coke}}$, m_{tar}, and m_{water} are the masses of semi-coke, tar, and water obtained at the current temperature stage, respectively (g); and $Y_{\text{gas+loss}}$, $Y_{\text{semi-coke}}$, Y_{tar}, and Y_{water} are the corresponding product yields (%).

2.3. Tar Separation and GC–MS Analysis

The condensable products generated during pyrolysis were collected using a condensation system to obtain the liquid products. The collected liquid products were allowed to stand at room temperature for 30 min to facilitate phase separation, and the tar phase was subsequently separated from the aqueous phase. For samples showing obvious emulsification, centrifugation at 3000 rpm for 10 min was applied to assist phase separation. The recovered tar samples were transferred into tightly sealed amber vials and stored at 4 °C prior to analysis to minimize the loss of low-boiling volatile components.

The volatile and semi-volatile organic components of the tar samples were analyzed using a GCMS-QP2010 SE gas chromatography–mass spectrometry system (Shimadzu, Japan) equipped with a static headspace sampling system. Approximately 1.00 g of each tar sample was placed in a 20 mL headspace vial, which was immediately sealed. The vial was equilibrated at 80 °C for 30 min, after which 1.0 mL of the headspace gas was introduced into the GC-MS system. The headspace sampling loop and transfer line temperatures were maintained at 100 and 120 °C, respectively. Chromatographic separation was performed using a DB-5 capillary column (30 m × 0.25 mm i.d. × 0.25 μm film thickness). High-purity helium (≥99.999%) was used as the carrier gas at a constant flow rate of 1.0 mL min^{-1}. The injector temperature was set at 250 °C, and the sample was introduced in split mode with a split ratio of 10:1. The oven temperature was initially maintained at 35 °C for 5 min, increased to 100 °C at 5 °C min^{-1}, and then further increased to 250 °C at 10 °C min^{-1}, followed by a final hold at 250 °C for 5 min. The total chromatographic run time was approximately 38 min. Mass spectrometric detection was performed in electron ionization (EI) mode at an ionization energy of 70 eV. The ion source and GC-MS interface temperatures were set at 200 and 250 °C, respectively. Mass spectra were acquired in full-scan mode over an m/z range of 35–550, with an event time of approximately 352 ms. Compound identification was carried out by comparing the experimentally obtained EI mass spectra with reference spectra in the NIST05, NIST14, and NIST21 mass spectral libraries. GC–MS compounds were tentatively identified by comparison with the NIST mass spectral library, using a similarity index (SI) ≥ 80 as the initial screening criterion. Peaks with ambiguous spectral assignments, conflicting chemical categories, or insufficient evidence for reliable classification were excluded from the compositional normalization but retained in the original peak records.

The relative abundance of each identified compound was estimated using the TIC peak-area normalization method according to the following:

$$A_i = \frac{S_i}{\sum_{j=1}^{n} S_j} \times 100\%$$

where A_i is the relative peak area of compound i(%); S_i is the integrated peak area of compound i; and $\sum S_j$ is the sum of the integrated areas of all valid peaks included in the analysis. Because different compounds exhibit different headspace partitioning behavior, volatility, chromatographic response, and mass spectrometric ionization efficiency, the

normalized peak-area percentages were used only to represent the relative abundance of detected components and should not be interpreted as their actual mass fractions in the tar. Based on molecular structural characteristics and potential utilization pathways, the identified compounds were classified into the following seven groups: (1) saturated aliphatic hydrocarbons; (2) unsaturated aliphatic hydrocarbons; (3) monocyclic aromatic hydrocarbons; (4) polycyclic aromatic hydrocarbons; (5) phenols; (6) other oxygen-containing compounds; (7) N/S-containing heteroatom compounds.

3. Results and Discussion

3.1. Pyrolysis Product Yields

Pyrolysis temperature plays an important role in determining the distribution of pyrolysis products from tar-rich coal [23–25,27]. The masses of pyrolysis products collected at different temperature stages under the two stress conditions are presented in Table 2, and the corresponding product yields are illustrated in Figure 3. As the temperature increased from 200 to 400 °C, the semi-coke yield of Baishihu tar-rich coal gradually decreased under both stress conditions. Under the no-external-stress condition, the tar yield increased with temperature, reaching 9.53% at 400 °C, and then gradually decreased at higher temperatures. In contrast, under the 15 MPa simulated formation stress condition, the tar yield exhibited a non-monotonic variation at relatively low temperatures, decreasing from 2.26% at 200 °C to 0.97% at 300 °C, followed by a sharp increase to a maximum of 8.81% at 400 °C. Therefore, although the detailed temperature-dependent behavior differed between the two stress conditions, the maximum tar yield occurred at approximately 400 °C in both cases. With a further increase in temperature, the tar yield gradually decreased, whereas the calculated semi-coke yield increased. It should be noted that the experiments were conducted using a staged continuous-heating pyrolysis procedure, and the semi-coke yield was calculated by difference and was therefore affected by the measured yields of the other products. Thus, the apparent increase in semi-coke yield at the later stages does not indicate an actual increase in the amount of solid residue; rather, the absolute amount of semi-coke continued to decrease throughout the overall pyrolysis process. With further increasing temperature, the gas + loss yield generally increased. Under the no-external-stress condition, the gas + loss yield increased from 0.06% at 200 °C to 7.01% at 700 °C. Under the 15 MPa simulated formation stress condition, the gas + loss yield reached a maximum of 7.86% at 600 °C and subsequently decreased to 1.41% at 700 °C. This variation indicates that, with increasing pyrolysis degree, some volatile intermediates may undergo further secondary cracking and convert into gaseous products [22]. However, the release process of products at high temperatures may still be affected by heat transfer within the lump coal specimen and volatile matter migration [32]. The water yield exhibited an increasing trend followed by a decreasing trend with increasing temperature and reached its maximum value at 300 °C. The formation of water during the low-temperature stage was mainly related to the release of adsorbed water in coal and the removal of oxygen-containing functional groups. With further temperature increase, the amount of releasable water and easily removed oxygen-containing structures in coal gradually decreased, resulting in a significant reduction in condensed water yield above 500 °C. This result indicates that water was no longer the dominant liquid-phase product during the high-temperature stage [33,34]. Under both stress conditions, the maximum tar yield occurred at the same pyrolysis temperature. However, noticeable differences in the distribution of certain products were observed across different temperature ranges, suggesting that simulated formation stress may also influence pyrolysis product distribution [22–26].

Table 2. Product masses collected during continuous pyrolysis of Baishihu tar-rich coal under different stress conditions.

Temperature Stage	Gas + Loss (g)	Water (g)	Tar (g)	Semi-Coke (g)
BS-C200 °C	0.7	75	1.7	1005.6
BS-C300 °C	1.8	130.1	10	863.7
BS-C400 °C	25.46	60	82.3	695.95
BS-C500 °C	31.14	0	28	636.79
BS-C600 °C	38.87	0	10.2	587.71
BS-C700 °C	41.21	0	2	544.5
BS-P200 °C	0.87	36.98	1.78	1066.88
BS-P300 °C	8.26	81.11	10.35	967.16
BS-P400 °C	42.8	36.9	85.18	802.28
BS-P500 °C	47.56	4.72	51.92	698.07
BS-P600 °C	54.86	1.57	16.21	625.43
BS-P700 °C	8.82	0	1.57	615.04

Note: BS-C denotes the no-external-stress condition, whereas BS-P denotes the 15 MPa simulated formation stress condition.

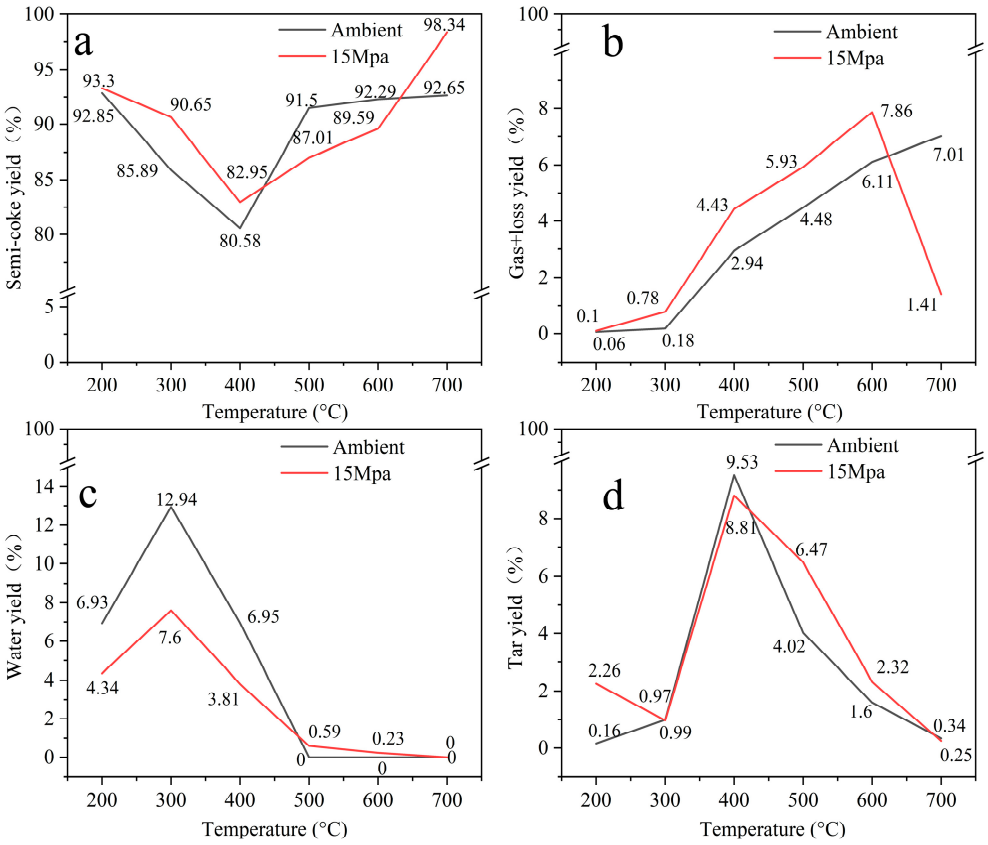


Figure 3. Changes in pyrolysis product yields at different temperatures under simulated formation-stress conditions: (**a**) semi-coke yield; (**b**) gas + loss yield; (**c**) water yield; and (**d**) tar yield.

3.2. Effect of Pyrolysis Temperature on Tar Composition

To further clarify the effect of pyrolysis temperature on tar composition, the tars obtained at 200–700 °C were analyzed by GC–MS. The GC–MS total ion chromatograms obtained at different pyrolysis temperatures are presented in Figure 4. Based on molecular structure and potential utilization attributes, valid components were classified into saturated aliphatic hydrocarbons, unsaturated aliphatic hydrocarbons, monocyclic aromatic hydrocarbons, polycyclic aromatic hydrocarbons, phenols, other oxygen-containing compounds, and

N/S-containing heteroatom compounds. The relative content of each group was calculated by normalizing the valid GC–MS peak areas (Tables S1 and 3). It should be noted that the relative intensity in the total-ion chromatograms represents within-sample normalization and is mainly used to show the distribution of peaks over the retention-time range, whereas temperature-dependent changes in compound classes were evaluated primarily using the normalized relative peak areas after classification. Overall, the tar composition exhibited three characteristic stages of evolution with increasing temperature.

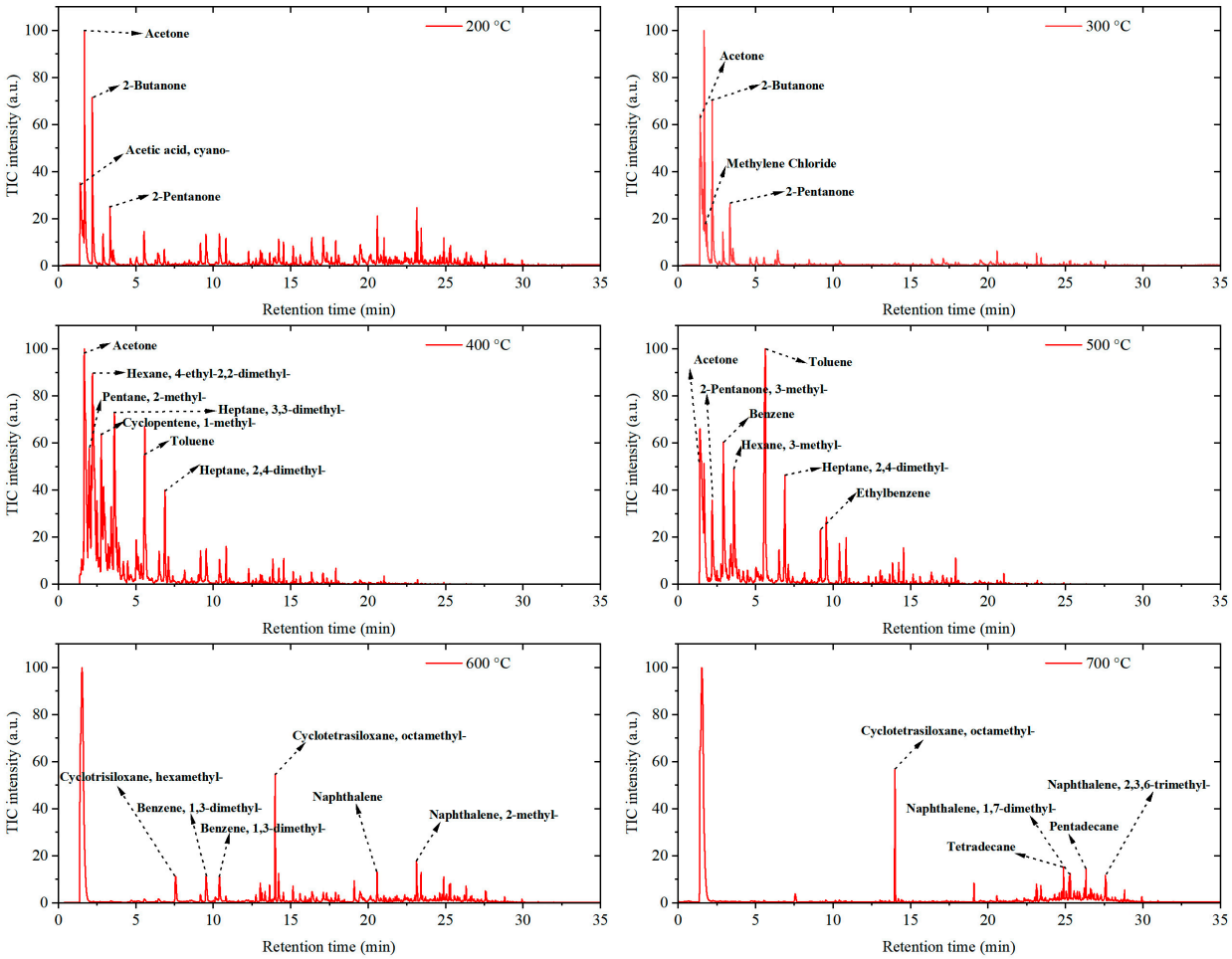


Figure 4. GC–MS total ion chromatograms of tar obtained at different pyrolysis temperatures under no external stress conditions.

The relative distributions of the major chemical groups at different pyrolysis temperatures are summarized in Figure 5. At the low-temperature stage of 200–300 °C, the tar mainly exhibited an enrichment of oxygen-containing compounds. At 200 °C, the relative peak area proportions of other oxygen-containing compounds and phenols were 43.97% and 9.31%, respectively. The relative GC–MS peak areas of acetone, 2-butanone, and 2-pentanone were 16.89%, 11.64%, and 4.72%, respectively. At 300 °C, the proportion of other oxygen-containing compounds further increased to 81.44%, with acetone, 2-butanone, and 2-pentanone reaching 31.8%, 23.05%, and 9.24%, respectively. The tar composition at this stage was mainly characterized by light carbonyl compounds, which may be associated with the cleavage of oxygen-containing functional groups in coal and the release of low-molecular-weight volatile products [27,33,34].

Table 3. Major representative compounds and relative contents in tar obtained at different pyrolysis temperatures.

Temp. (°C)	Compound	Category	Norm. TIC Area (%)	Temp. (°C)	Compound	Category	Norm. TIC Area (%)
200	Acetone	Other oxygenates	16.89	500	Toluene	Monocyclic aromatics	19.62
200	2-Butanone	Other oxygenates	11.64	500	Benzene	Monocyclic aromatics	9.16
200	2-Pentanone	Other oxygenates	4.72	500	Acetone	Other oxygenates	8.15
200	Ethyl alcohol	Other oxygenates	3.54	500	Hexane, 3-methyl-	Saturated aliphatics	7.65
200	Toluene	Monocyclic aromatics	3.13	500	2-Pentanone, 3-methyl-	Other oxygenates	5.89
200	Naphthalene	Polycyclic aromatics	2.95	500	Heptane, 2,4-dimethyl-	Saturated aliphatics	5.79
300	Acetone	Other oxygenates	31.80	500	Benzene, 1,3-dimethyl-	Monocyclic aromatics	4.29
300	2-Butanone	Other oxygenates	23.05	600	Benzene, 1,3-dimethyl-	Monocyclic aromatics	6.36
300	2-Pentanone	Other oxygenates	9.24	600	Benzene, 1,3,5trimethyl-	Monocyclic aromatics	4.39
300	2-Butanone, 3-methyl-	Other oxygenates	5.11	600	Naphthalene	Polycyclic aromatics	3.60
300	2-Hexanone	Other oxygenates	2.77	600	Naphthalene, 2-methyl-	Polycyclic aromatics	3.22
300	3-Pentanone	Other oxygenates	2.75	600	Benzene, 1-ethyl-2-methyl-	Monocyclic aromatics	2.22
400	Acetone	Other oxygenates	13.57	600	Naphthalene, 1,4-dimethyl-	Polycyclic aromatics	1.74
400	Heptane,3,3-dimethyl-	Saturated aliphatics	7.42	700	Tetradecane	Saturated aliphatics	6.16
400	Hexane, 4-ethyl-2,2-dimethyl-	Saturated aliphatics	5.73	700	Naphthalene, 1,7-dimethyl-	Polycyclic aromatics	5.07
400	Toluene	Monocyclic aromatics	5.34	700	Naphthalene, 2,3,6trimethyl-	Polycyclic aromatics	4.83
400	Cyclopentene, 1-methyl-	Unsaturated aliphatics	9.19	700	Pentadecane	Saturated aliphatics	4.61
400	Pentane, 2-methyl-	Saturated aliphatics	4.55	700	Naphthalene, 1,4-dimethyl-	Polycyclic aromatics	3.53
400	Benzene	Monocyclic aromatics	3.85	700	Naphthalene, 2-methyl-	Polycyclic aromatics	2.89
				700	Naphthalene, 1,5-dimethyl-	Polycyclic aromatics	2.14

When the temperature increased to 400 °C, the tar composition changed markedly. The relative peak area proportions of saturated and unsaturated aliphatic hydrocarbons reached 35.18% and 29.82%, respectively, with a total proportion of 65%, making them the dominant components at this temperature. Meanwhile, the proportion of other oxygen-containing compounds decreased to 19.49%. GC–MS detected large amounts of aliphatic and cyclic hydrocarbons, including 3,3-dimethylheptane (7.42%), a branched hexane (5.73%), and 1-methylcyclopentene (9.19%), while benzene and toluene reached 3.85% and 5.34%, respectively. These results indicate that 400 °C is the principal stage for substantial formation

of aliphatic hydrocarbons. When the temperature increased to 500 °C, the relative content of monocyclic aromatic hydrocarbons increased rapidly from 14.26% at 400 °C to 41.23%, whereas the total aliphatic-hydrocarbon content decreased from 65% to 40.88%. These results indicate that tar obtained at 500 °C exhibited clear enrichment of light monocyclic aromatic hydrocarbons. This change may be related to the further dehydrogenation, cyclization, and aromatization of aliphatic intermediates, resulting in the conversion of some non-aromatic structures into benzene-series aromatic structures [27,34].

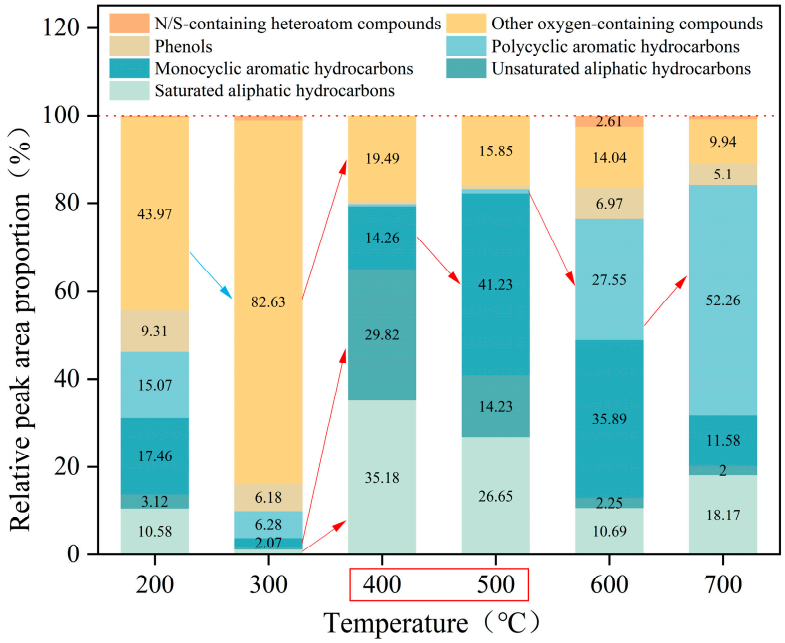


Figure 5. Relative contents of the major chemical groups in tar obtained at different pyrolysis temperatures.

During the high-temperature stage (600–700 °C), the distribution of the retained GC-MS signals shifted toward compounds classified as polycyclic aromatics. At 600 °C, monocyclic and polycyclic aromatics accounted for 35.89% and 27.55% of the normalized TIC peak area, respectively, with a combined proportion of 63.44%. At 700 °C, the combined proportion remained relatively stable at 63.84%, while monocyclic aromatics decreased to 11.58% and polycyclic aromatics increased to 52.26%, indicating that high temperature mainly promoted the conversion of aromatic components from monocyclic to condensed-ring structures [34]. It should be noted that the retained peaks accounted for only 37.61% and 23.67% of the total integrated TIC peak areas at 600 and 700 °C, respectively. This limited coverage was primarily attributed to intense early-eluting signals dominated by m/z 44 with ambiguous library assignments, together with other peaks that could not be reliably classified. Therefore, the observed trend indicates a relative enrichment of polycyclic aromatic compounds among the retained GC–MS signals rather than an absolute increase in their content in the whole tar (Supplementary Table S1). Overall, Baishihu tar-rich coal tar was dominated by light oxygen-containing compounds below 300 °C, was richest in aliphatic hydrocarbons at 400 °C, showed pronounced enrichment of monocyclic aromatics at 500 °C, and progressively evolved toward polycyclic aromatic structures at 600–700 °C. These results demonstrate that pyrolysis temperature affects not only tar yield but also tar composition and its potential utilization route.

3.3. Changes in Tar Composition Under Simulated Formation Stress

To assess the effect of simulated formation stress on tar composition, GC–MS analyses were conducted on tars produced at 400 °C, the temperature corresponding to the maximum tar yield, under no external stress and 15 MPa simulated formation stress. The GC–MS results and compositional classification data are presented in Figure 6 and Supplementary Table S1, while changes in representative compounds are summarized in Table 4. According to the classification results shown in the Figure 6, under the no-external-stress condition, the relative peak area proportions of saturated and unsaturated aliphatic hydrocarbons were 35.18% and 29.82%, respectively, with a total proportion of 65%. Under the 15 MPa condition, these values decreased to 30.05% and 22.02%, respectively, with the total proportion decreasing to 52.07%, representing a reduction of 12.93 percentage points. Among them, saturated aliphatic hydrocarbons showed a greater decrease, indicating that the relative proportion of aliphatic hydrocarbons in the recovered tar decreased under mechanical stress conditions. Although the overall proportion of aliphatic hydrocarbons decreased, the tar obtained under stress conditions still contained abundant heptane, branched alkanes, and alkenes.

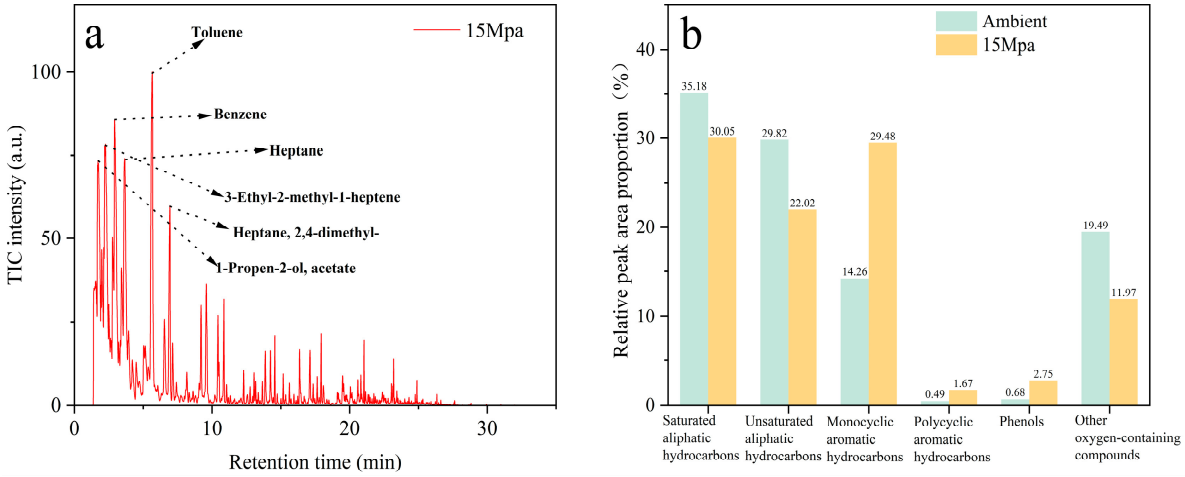


Figure 6. Effect of simulated formation stress on tar composition at 400 °C: (**a**) GC–MS total ion chromatogram of tar obtained under 15 MPa simulated formation stress; (**b**) relative contents of the major chemical groups under different stress conditions.

Compared with the decrease in aliphatic hydrocarbons, simulated formation stress was more strongly associated with a higher relative proportion of aromatic compounds in the recovered tar. The relative peak area proportion of monocyclic aromatic hydrocarbons increased from 14.26% under no external stress to 29.48%, an increase of 15.22 percentage points, while polycyclic aromatic hydrocarbons increased from 0.49% to 1.67%. Consequently, the total aromatic-hydrocarbon content increased from 14.75% to 31.15%, nearly doubling, and the increase was derived mainly from monocyclic aromatics. Specifically, the original relative peak areas of benzene and toluene increased from 3.85% and 5.34% under no external stress to 9.81% and 11.03% under 15 MPa simulated formation stress, respectively. Ethylbenzene increased from 0.95% to 1.67%, m-xylene from 1.16% to 2.56%, and o-xylene from 0.58% to 1.11%. When benzene, toluene, ethylbenzene, m-xylene, and o-xylene were considered together, their total relative peak area increased from approximately 11.88% to 26.18%, indicating that simulated formation stress was particularly favorable for enriching light monocyclic aromatic compounds in the tar.

Table 4. Major representative compounds and relative contents in tar at 400 °C under different stress conditions.

Compound	Category	No External Stress (%)	15 MPa (%)	Change (Percentage Points)
Cyclopentene, 1-methyl-	Unsaturated aliphatics	4.89	3.60	−1.29
Pentane, 2-methyl-	Saturated aliphatics	4.55	3.19	−1.36
Heptane, 2,4-dimethyl-	Saturated aliphatics	2.95	3.96	+1.01
Benzene	Monocyclic aromatics	3.85	9.81	+5.96
Toluene	Monocyclic aromatics	5.34	11.03	+5.69
Ethylbenzene	Monocyclic aromatics	0.95	1.67	+0.71
Benzene, 1,3-dimethyl-	Monocyclic aromatics	1.16	2.56	+1.40
o-Xylene	Monocyclic aromatics	0.58	1.11	+0.52

In addition, simulated formation stress also altered the distribution of oxygen-containing compounds. Under the no-external-stress condition, the relative peak area proportion of other oxygen-containing compounds was 19.66%, which decreased to 11.97% under the 15 MPa condition, whereas phenolic compounds increased from 0.68% to 2.75%. These results indicate that mechanical stress did not cause all oxygen-containing compounds to exhibit the same variation trend but resulted in selective redistribution among different oxygen-containing compound categories. Combined with the yield results in Section 3.1, simulated formation stress at 400 °C slightly decreased tar yield from 9.53% to 8.81%, while the relative peak area proportion of aromatic hydrocarbons in tar increased from 14.75% to 31.15%. These results indicate that the effect of simulated formation stress is reflected not only in changes in tar yield but, more importantly, in redistribution of the liquid-product composition. A possible explanation is that external mechanical stress alters the pore–fracture structure of the coal and the transport conditions of volatile products, increasing the residence and contact times of some primary pyrolysis products within the coal matrix. This may enhance secondary reactions such as cyclization, dehydrogenation, and aromatization of reactive intermediates such as alkenes, ultimately decreasing the relative content of aliphatic hydrocarbons while enriching monocyclic aromatic hydrocarbons such as benzene and toluene [15,16,22,25,26].

3.4. Fractionated Utilization of Baishihu Coal Tar and Implications for In Situ Pyrolysis

Baishihu tar-rich coal pyrolysis tar contains aliphatic hydrocarbons, monocyclic aromatic hydrocarbons, polycyclic aromatic hydrocarbons, phenols, and other oxygen-containing compounds, and the dominant component groups differ markedly with pyrolysis temperature. Therefore, compared with treating the entire tar as a single liquid product, fractionated and graded utilization based on the compositional characteristics at different temperatures is more conducive to realizing the potential value of the individual tar components [7,8]. It should be emphasized that the GC–MS results primarily reflect the relative peak areas of detected headspace components rather than the actual mass fractions of the bulk tar. Furthermore, as the pyrolysis experiments were not independently replicated, the observed trends should be interpreted cautiously without implying statistical significance. Accordingly, the utilization routes discussed below are intended as a preliminary assessment based primarily on the detected chemical composition (Figure 7).

Practical engineering applications should additionally consider boiling range, viscosity, density, heating value, acid value, and hydrotreating performance.

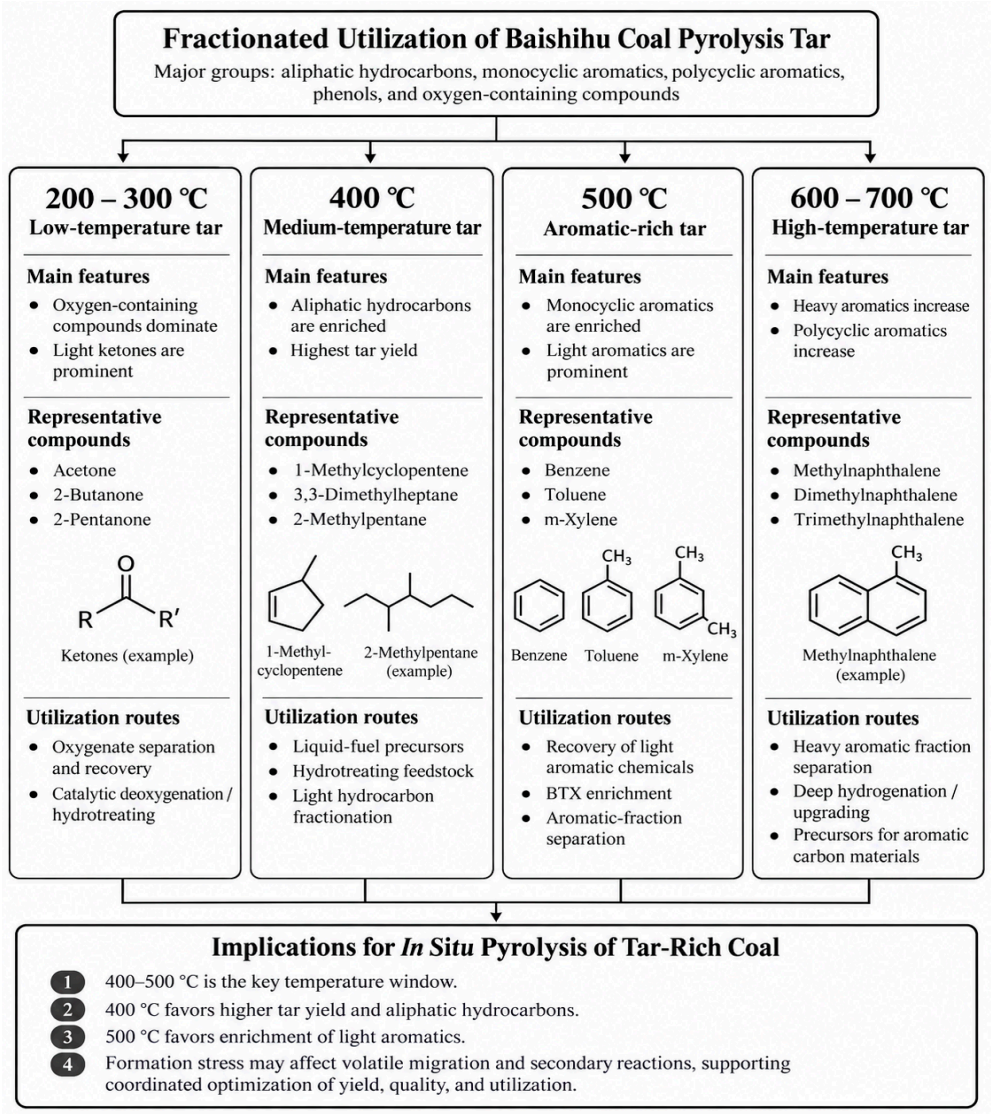


Figure 7. Fractionated utilization pathways for Baishihu coal tar.

The tar obtained at 200–300 °C exhibited obvious enrichment of oxygen-containing compounds, with ketones and other light oxygen-containing components dominating the liquid products during the low-temperature stage. Such components may have potential for separation and recovery as oxygenated chemicals; however, a high oxygen content can also impair the stability and downstream processing performance of tar as a liquid-fuel feedstock. Therefore, low-temperature tar is more suitably considered for oxygenate separation, catalytic deoxygenation, or hydrotreating rather than being regarded directly as a high-quality fuel oil [8,35]. At 400 °C, Baishihu tar-rich coal achieved the maximum tar yield, while aliphatic hydrocarbons exhibited a relatively high relative peak area proportion in the tar. Saturated and unsaturated aliphatic hydrocarbons together constituted the major components of tar, indicating that the tar obtained at this temperature exhibited pronounced hydrocarbon characteristics. From the perspective of composition, the tar obtained at 400 °C has potential to be evaluated as a fuel precursor or feedstock for further hydro-upgrading processes [8,34]. When the temperature increased to 500 °C, the tar composition further evolved toward aromatization, with a clear increase in the proportion of monocyclic aromatic

hydrocarbons. Light aromatic components, including benzene, toluene, ethylbenzene, and xylenes, showed relative enrichment. Compared with 400 °C, the tar yield at 500 °C decreased, while the proportion of aromatic components increased. Therefore, based on its compositional characteristics, tar obtained at 500 °C may serve as a potential research target for the separation and further catalytic conversion of light aromatic components, providing a reference for the targeted utilization of aromatic chemicals [7,35–38]. These results suggest that 400 °C is more favorable when liquid product yield is the primary objective, whereas 500 °C provides greater potential for targeted regulation of products with emphasis on light aromatic chemicals.

The simulated formation-stress experiments further indicate that, in addition to temperature, the coal-seam stress environment may provide another means of regulating tar composition. From the perspective of in situ pyrolysis of tar-rich coal, underground development should not focus solely on maximizing total tar yield, but should also consider tar quality and targeted enrichment of desired components. Considering both tar yield and composition, 400–500 °C can be regarded as a temperature range deserving particular attention for in situ pyrolysis of Baishihu tar-rich coal. A temperature of 400 °C is more favorable for obtaining higher tar yields and aliphatic-hydrocarbon components, whereas 500 °C is more favorable for enriching light monocyclic aromatics. The marked increase in light aromatic components under simulated formation stress also suggests that the stress environment in actual coal seams may further alter tar composition and quality by influencing volatile transport and secondary reactions. Future studies could therefore consider multiple formation-stress levels, heating rates, and pore–fracture evolution to investigate in situ pyrolysis under coupled thermo-mechanical–seepage conditions [15,16,25,26]. Additional characterization of boiling range, viscosity, stability, and hydrotreating performance would also help move the optimization of tar-rich coal in situ pyrolysis from a sole focus on oil-and-gas yield toward coordinated optimization of “yield–quality–utilization route”.

4. Conclusions

(1) Pyrolysis temperature was the primary factor controlling the distribution of pyrolysis products from Baishihu tar-rich coal. Tar yield reached maximum values at 400 °C with increasing temperature, reaching maxima of 9.53% and 8.81% at 400 °C under no external stress and 15 MPa simulated formation stress, respectively. This result indicates that 400 °C represents the temperature stage with the highest tar yield under the experimental conditions.

(2) Tar composition exhibited a clear stagewise evolution with increasing temperature: oxygen-containing compounds were relatively enriched at 200–300 °C; aliphatic hydrocarbons were characterized by a high relative peak area proportion at 400 °C; monocyclic aromatic hydrocarbons showed a high relative peak area proportion (41.11%) at 500 °C; and the tar progressively evolved toward polycyclic aromatic structures at 600–700 °C. Overall, these results indicate that pyrolysis temperature regulates the chemical composition and evolution characteristics of tar.

(3) A simulated formation stress of 15 MPa altered the composition of tar produced at 400 °C, decreasing the relative peak area proportion of aliphatic hydrocarbons while increasing aromatic hydrocarbons from 14.80% to 28.82%, with pronounced enrichment of light monocyclic aromatics. Considering both tar yield and composition characteristics, 400–500 °C represents a temperature range of particular interest for Baishihu tar-rich coal pyrolysis. A temperature of 400 °C is favorable for obtaining a higher tar yield, whereas 500 °C is favorable for the relative enrichment of light aromatic components. These findings provide experimental insights into tar composition evolution under simulated formation stress conditions.

Supplementary Materials: The following supporting information can be downloaded at https://www.mdpi.com/article/10.3390/pr14213549/s1. File S1: Raw GC–MS data and corresponding mass spectral library matching results for coal tar samples; Table S1: Classification of coal tar components and calculation of their relative peak area percentages based on GC–MS data.

Author Contributions: The conceptualization and methodology were conducted by H.C. and W.W.; the investigation and analysis were conducted by H.C. and H.S.; writing was conducted by H.C.; review and editing were conducted by H.S. All authors have read and agreed to the published version of the manuscript.

Funding: This research was supported by the Natural Science Foundation of China (42472236), the Xinjiang Uygur Autonomous Region Introduction Plan "Tianchi Talent" project (Grant No. 5105250180k), the Key Program of the Natural Science Foundation of Xinjiang Uygur Autonomous Region (No.2025D01D14), the Henan Provincial Natural Science Foundation (262300421765), and the Innovative and Expanded Talent Program for Intellectual Support to Xinjiang: Jiangsu Province Coal-Based Solid Waste Resource Utilization "Support Group for Xinjiang" (Document No. [2024]16), and the Major Science and Technology Special Project of Xinjiang Uygur Autonomous Region (Grant No. 2022A03014).

Data Availability Statement: The data supporting this study are provided in the article and the Supplementary Materials. File S1 contains the original total ion chromatograms (TICs) of tar samples under all experimental conditions, together with compound identification results obtained by comparison with the NIST mass spectral library. Supplementary Table S1 provides the underlying data used for compound classification and peak-area normalization calculations. The compound identification and normalization datasets represent processed chromatographic peak-level information.

Acknowledgments: We are grateful to all the editors and reviewers who have helped us to improve and publish this paper.

Conflicts of Interest: The authors declare no conflicts of interest.

References

1. Wang, P.; Wen, F.; Bu, X.; Liu, Y.; Bian, W.; Deng, Y. Study on the Pyrolysis Characteristics of Coal. *Coal Convers*. **2005**, *28*, 8–13. (In Chinese)
2. Wang, S.; Shi, Q.; Wang, S.; Shen, Y.; Sun, Q.; Cai, Y. Resource Property and Exploitation Concepts with Green and Low-Carbon of Tar-Rich Coal as Coal-Based Oil and Gas. *J. China Coal Soc*. **2021**, *46*, 1365–1377. (In Chinese)
3. Wang, S.; Wang, H.; Ren, S.; Dong, S.; Zheng, D.; Tan, K.; Hou, E.; Wang, S.; Qu, Y.; Jiao, X. Potential Analysis and Technical Conception of Exploitation and Utilization of Tar-Rich Coal in Western China. *Strategy Study CAE* **2022**, *24*, 49–57. (In Chinese) [CrossRef]
4. Wang, S.; Bao, Y.; Hao, Y.; Wang, S.; Shi, Q.; Li, D.; Hu, Y. Research on Tar-Rich Coals: Progress and Prospects. *Coal Geol. Explor.* **2024**, *52*, 2. (In Chinese)
5. Fu, D.; Duan, Z.; Yang, F.; Ma, L.; Wang, Z.; Tian, T.; He, D. Key Problems in In Situ Pyrolysis of Tar-Rich Coal Drilling for Extraction of Coal-Based Oil and Gas Resources. *J. China Coal Soc*. **2023**, *48*, 1759–1772. (In Chinese)
6. Ma, L.; Duan, Z.; Yang, F.; Fu, D.; Wang, Z. Study on the Significance of Coal In Situ Underground Pyrolytic Oil Production under Carbon Peaking and Carbon Neutrality Background. *Coal Geol. China* **2022**, *34*, 5–7. (In Chinese)
7. Manera, C.; Fragoso, H.P.; Agra, A.A.; Flores, B.D.; Osório, E.; Godinho, M.; Vilela, A.C.F. Systematic Mapping of Studies on Coal Tar and Pitch over the Last Five Decades (1970–2023). *Chem. Eng. Res. Des*. **2023**, *196*, 427–450. [CrossRef]
8. Deng, J.; Lang, W.; Ouyang, J.; Li, Z.; Yuan, S. Catalytic Upgrading of Coal Tar to Produce Value-Added Chemicals and Fuels: A Review on Processes, Catalytic Mechanisms and Catalysts. *Chem. Eng. J*. **2024**, *500*, 157420. [CrossRef]
9. Zhang, H.R.; Li, S.; Kelly, K.E.; Eddings, E.G. Underground In Situ Coal Thermal Treatment for Synthetic Fuels Production. *Prog. Energy Combust. Sci*. **2017**, *62*, 1–32. [CrossRef]
10. Dong, G.; Zhu, C.; Li, J.; Xu, S.; Guo, W. Numerical Simulation on Development Effect of Tar-Rich Coal through In Situ Conversion by Convective Heating in Huangling Mining Area. *Coal Geol. Explor.* **2023**, *51*, 57–67. (In Chinese)

11. Ju, Y.; Zhu, Y.; Zhou, H.; Ge, S.; Xie, H. Microwave Pyrolysis and Its Applications to the In Situ Recovery and Conversion of Oil from Tar-Rich Coal: An Overview on Fundamentals, Methods, and Challenges. *Energy Rep*. **2021**, *7*, 523–536. [CrossRef]
12. Ju, Y.; Zhu, Y.; Zhang, Y.; Zhou, H.; Peng, S.; Ge, S. Effects of High-Power Microwave Irradiation on Tar-Rich Coal for Realising In Situ Pyrolysis, Fragmentation, and Low-Carbon Utilisation of Tar-Rich Coal. *Int. J. Rock Mech. Min. Sci*. **2022**, *157*, 105165. [CrossRef]
13. Ju, Y.; Zhu, Y.; Zhang, Y.; Iglauer, S.; Pan, B.; Wang, K. Microwave-Aided Pyrolysis and Fragmentation of Tar-Rich Coal and Rocks for In Situ Coal Conversion and Clean Utilization. *Int. J. Rock Mech. Min. Sci*. **2023**, *167*, 105391. [CrossRef]
14. Tang, Y.; Wu, X.; Li, L.; Su, Z.; Wang, R. Heating Technology of In Situ Pyrolysis for Tar-Rich Coal and Its High-Efficiency Process. *Clean Coal Technol*. **2023**, *29*, 42–50. (In Chinese)
15. Zhao, Y.; Qu, F.; Wan, Z.; Zhang, Y.; Liang, W.; Meng, Q. Experimental Investigation on Correlation between Permeability Variation and Pore Structure during Coal Pyrolysis. *Transp. Porous Media* **2010**, *82*, 401–412. [CrossRef]
16. Shi, J.; Feng, Z.; Zhou, D.; Li, X.; Meng, Q. Analysis of the Permeability Evolution Law of In Situ Steam Pyrolysis of Bituminous Coal Combining with In Situ CT Technology. *Energy* **2023**, *263*, 126009. [CrossRef]
17. Yan, H.; Zhang, X.; Xu, K.; Li, H.; Xu, J.; Wang, Y.; Jiang, L.; Su, S.; Hu, S.; Xiang, J. Effect of Pressure on the Structure and Combustion Reactivity of Pyrolytic Coal Char. *Clean Coal Technol*. **2021**, *27*, 68–76. (In Chinese)
18. Wu, J.; Di, Z.; Luo, M.; Wang, Y.; Ding, X.; Li, H. Study of the Effects of Temperature and Pressure on Coal Pyrolysis in an N_2 Atmosphere. *Chem. Ind. Eng. Prog*. **2019**, *38*, 116–121. (In Chinese)
19. Li, X.; Cen, J.; Xia, Z.; Fang, M.; Wang, T.; Wang, Q.; Luo, Z. Pressurized Pyrolysis Characteristics of Pine Sawdust and Coal. *J. Zhejiang Univ. Eng. Sci*. **2019**, *53*, 1298–1305. (In Chinese)
20. Wang, N.; Huang, Y.; Liu, Q.; Zhang, Y.; Yang, H. Effects of Pyrolysis Conditions on Pressurized Pyrolysis of Xiwan Coal in a Fluidized Bed. *Coal Convers*. **2021**, *44*, 34–43. (In Chinese)
21. Deng, L.; Sun, S.; Zhang, W.; Bai, C.; Feng, D.; Zhao, Y.; Wu, Q. Effects of Pressure on Coal Pyrolysis Process and Physicochemical Structure of Pyrolysis Char. *J. Combust. Sci. Technol*. **2021**, *27*, 644–652. (In Chinese)
22. Shi, Q.; Shi, Y.; Wang, S.; Kou, B.; Zhao, H.; Ji, R.; Yang, X.; Liu, P.; Li, Z. Experimental Study on the Tar and Gas Distribution during Tar-Rich Coal Pyrolysis with Stress Loading. *Fuel* **2024**, *376*, 132727. [CrossRef]
23. Ning, X.; Huang, X.; Xue, X.; Wang, C.; Deng, L.; Che, D. Experimental Study on Yield and Quality of Tar from Tar-Rich Coal under Simulated In Situ Conditions. *J. Energy Inst*. **2025**, *118*, 101912. [CrossRef]
24. Chen, M.; Wang, C.; Yuan, T.; Ning, X.; Huang, X.; Deng, L.; Che, D. Experimental Investigation on Gas–Liquid–Solid Three-Phase Product Distributions during the Simulated In Situ Pyrolysis of Tar-Rich Coal. *Fuel* **2025**, *381*, 133465. [CrossRef]
25. Chen, M.; Du, Y.; Wang, C.; Yuan, T.; Hou, Y.; Chang, L.; Deng, L.; Che, D. Study on Characterization of Three-Phase Products and Microstructure Evolution during In Situ Pyrolysis of Tar-Rich Coal at Different Temperatures. *Fuel* **2025**, *388*, 134562. [CrossRef]
26. Kou, B.; Shi, Q.; Wang, S.; Cui, S.; Li, C.; Yang, X.; Shi, Y.; Zhao, X.; Zheng, J.; Ma, L. Investigation on the Influence of Macrolithotypes on the Tar-Rich Coal In Situ Pyrolysis Behavior. *Fuel* **2026**, *412*, 138147. [CrossRef]
27. Shi, Q.; Mi, Y.; Wang, S.; Cai, Y.; Ji, R.; Xue, W.; Li, X.; Han, B. Pyrolysis Behavior of Tar-Rich Coal with Various Coal-Forming Environments: A TGA and In Situ Transmission FTIR Study. *Fuel* **2024**, *358*, 130250. [CrossRef]
28. Shi, Q.; Li, C.; Wang, S.; Ji, R.; Xue, W.; Mi, Y.; Wang, S.; Cai, Y. Variation of Molecular Structures Affecting Tar Yield: A Comprehensive Analysis on Coal Ranks and Depositional Environments. *Fuel* **2023**, *335*, 127050. [CrossRef]
29. Zhang, L.; Shi, J.; Zhang, D.; Ning, S.; Zhang, J.; Lin, Z.; Sun, J.; Huang, S.; Zou, Z.; Liu, K.; et al. Coal Petrology and Coal Quality Characteristics in the Baishihu Mining Area of Naomaohu, Xinjiang. *Coal Geol. China* **2022**, *34*, 15–22. (In Chinese)
30. *GB/T 212-2008*; Proximate Analysis of Coal. Standards Press of China: Beijing, China, 2008.
31. *GB/T 476-2008*; Determination of Carbon and Hydrogen in Coal. Standards Press of China: Beijing, China, 2008.
32. Luo, Y.; Liu, L.; Lv, L.; Zhang, S.; Dai, F.; Jin, H.; Sui, J. Moderate-temperature pyrolysis characteristics of lump coal under varying coal particle sizes. *Energies* **2025**, *18*, 3220. [CrossRef]
33. Zhou, Y. In Situ Characterization of Pyrolysis Characteristics and Reaction Mechanism of Low-Rank Coal. Ph.D. Thesis, Dalian University of Technology, Dalian, China, 2019. (In Chinese)
34. Wang, Q.; Wang, M.; Wang, H.; Kong, J.; Xie, W.; Wang, J.; Chang, L.; Bao, W. Effect of Temperature and Gasification Gas from Char on the Reactions of Volatiles Generated from Rapid Pyrolysis of a Low-Rank Coal. *Fuel Process. Technol*. **2021**, *212*, 106601. [CrossRef]
35. Bei, P.; Zhao, J.; Xu, X.; Yi, L.; Deng, L.; Li, W. Separation of Value-Added Chemicals from Coal Tar: Mechanisms, Advances, and Perspectives. *Fuel* **2026**, *418*, 138750. [CrossRef]
36. Huang, R.; Yuan, X.; Yan, L.; Han, L.; Bao, W.; Chang, L.; Liu, J.; Wang, J.; Ok, Y.S. Carbon Precursors in Coal Tar: Extraction and Preparation of Carbon Materials. *Sci. Total Environ*. **2021**, *788*, 147697. [CrossRef] [PubMed]

37. Banerjee, C.; Chandaliya, V.; Dash, P.S. Recent Advancement in Coal Tar Pitch-Based Carbon Fiber Precursor Development and Fiber Manufacturing Process. *J. Anal. Appl. Pyrolysis* **2021**, *158*, 105272. [CrossRef]
38. Yang, Y.; Li, Z.; Qu, S. Structural Engineering of Pitch-Based Porous Carbon and Its Application in Supercapacitors: A Review. *J. Energy Storage* **2023**, *74*, 109334. [CrossRef]

Disclaimer/Publisher's Note: The statements, opinions and data contained in all publications are solely those of the individual author(s) and contributor(s) and not of MDPI and/or the editor(s). MDPI and/or the editor(s) disclaim responsibility for any injury to people or property resulting from any ideas, methods, instructions or products referred to in the content.